

## Characterizations and Surface Wettability of Fluorinated Block Copolymers Synthesized by Atom Transfer Radical Polymerization

Masaya HIKITA<sup>1</sup>, Norikazu TAKIZUKA<sup>2</sup>, Keiji TANAKA<sup>3</sup>,  
Atsushi TAKAHARA<sup>4</sup>, and Tisato KAJIYAMA<sup>5</sup>

<sup>1</sup>Japan Chemical Innovation Institute, JAPAN, <sup>2</sup>NOF Corp., JAPAN, <sup>3</sup>Graduate School of Engineering, Kyushu University, JAPAN, <sup>4</sup>Institute for Materials Chemistry and Engineering, Kyushu University, JAPAN, <sup>5</sup>Kyushu University, JAPAN

Kyushu University, 6-10-1 Hakozaki, Higashi-ku, Fukuoka 812-8581, JAPAN

Tel: +81-92-642-4385, Fax: +81-92-651-5606, m-hikita@cstf.kyushu-u.ac.jp

Poly(styrene-*block*-2-perfluorooctyl ethyl acrylate) [P(St-*b*-PFA)] diblock copolymers were synthesized by atom transfer radical polymerization (ATRP). Films of P(St-*b*-PFA) with various PFA contents were structurally characterized, from bulk to surface. X-ray diffraction measurement and transmission electron microscopic observation revealed that the internal bulk region of the P(St-*b*-PFA) film was in a microphase-separated state. Also, X-ray photoelectron spectroscopy showed that the surface in the P(St-*b*-PFA) films was covered with the PFA layer, and that the layer thickness became thicker with increasing PFA content. Surface wettability for the P(St-*b*-PFA) films was studied by dynamic contact angle measurement. In the case of the P(St-*b*-PFA) films with the PFA content higher than 20 mol %, the contact angles to water and dodecane were 120 and 76 degree, respectively, with almost no hysteresis. These excellent water and oil repellencies are closely related to the stable surface layer of PFA groups, which might prevent from reconstructing the surface structure. In contrast, the intriguing liquid repellent properties were not observed at all for the random copolymers in which the clear surface PFA layer was not formed.

Key words: atom transfer radical polymerization, fluorinated block copolymers, surface wettability

### 1. INTRODUCTION

Fluorinated polymer is a class of versatile polymeric materials with potential applications<sup>1</sup>. Incorporation of fluorine atoms to a polymer renders its surface energy substantially lower, resulting in chemically inactive surface. Such leads to low wettability with usual liquids and thus low adhesion properties.

So far, surface properties of fluorinated block and random copolymers have been extensively studied. Consequently, it has been accepted that the distribution of fluorinated segments greatly affects on its surface activities. Hence, controlling the distribution of fluorinated segments is of importance as the first benchmark to design and construct highly-functionalized fluorinated polymers. From this point of view, *block* copolymers containing fluorinated segments should be excellent because such the lower surface energy segments can be efficiently partitioned to the surface to form a surface phase-separated domain. Many kinds of block copolymers have been hitherto synthesized using variable methods, and the relation of the orientation of fluorinated block to the surface properties has been studied. Wang and co-workers synthesized fluorinated diblock copolymers by polymer analogous reaction of poly(styrene-*block*-isoprene) with perfluoroalkyl acid chloride<sup>2</sup>. The obtained copolymers with the side chains of (CF<sub>2</sub>)<sub>6</sub> group, or longer, exhibited an excellent water repellency such as 120 and 109 degrees as advancing and receding contact angles, respectively. They claimed that

the perfluoroalkyl groups form a mesogen-like structure of liquid crystalline at the surface, as well as in the bulk, which might prevent from reconstructing the surface structure.

In this study, we first synthesize well-defined poly(styrene-*block*-2-perfluorooctyl ethyl acrylate) [P(St-*b*-PFA)] copolymers with various chemical compositions by ATRP<sup>3</sup>, and characterize bulk and surface structures in films of P(St-*b*-PFA). Then, surface wettability of the films against to water and oil are examined.

### 2. EXPERIMENTAL

#### 2.1. Polymerization procedures

Fig. 1 shows the synthetic route for P(St-*b*-PFA). At first, macroinitiators **1** were prepared by bulk ATRP reactions under typical conditions. Next, P(St-*b*-PFA) copolymers **2** were synthesized in solutions under typical ATRP conditions at 373 K for a given polymerization time. Since the relationship between  $M_{n,cal}$  and conversion was linear, it was judged that the polymerization proceeded in the living manner. Actually, this enables us to regulate the PFA content in the copolymers by changing the polymerization time. Also, random copolymers [P(St-*ran*-PFA)] were also synthesized by a conventional free radical polymerization using 2,2'-azobisisobutyronitrile (AIBN) as an initiator in 2-butanone at 343K for 8h. Aggregation states and surface wettability of the P(St-*b*-PFA) films are compared with those of the P(St-*ran*-PFA) films. Table I shows the list of diblock and random copolymers.

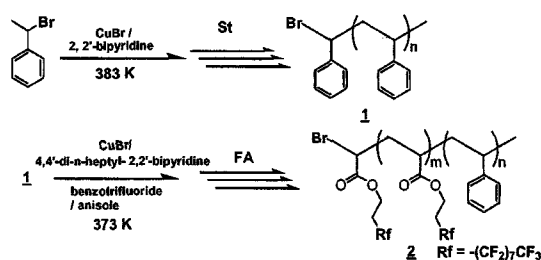


**Fig.1** Synthetic scheme of P(St-b-PFA) diblock copolymer by ATRP.

**Table I** Characterizations of P(St-b-PFA) by ATRP and P(St-*ran*-PFA) by free radical polymerization.

samples	$M_{n,cal}$ <sup>1)</sup>	$M_w/M_n$ <sup>2)</sup>	PFA molar ratio
b-1	10,000	1.21	7.6
b-2	12,700	1.22	13.8
b-3	15,200	1.24	18.7
b-4	21,700	1.25	29.3
b-5	25,700	1.22	34.6
r-1	27,700 <sup>2)</sup>	1.70	6.9
r-2	23,200 <sup>2)</sup>	1.56	21.0
r-3	25,700 <sup>2)</sup>	1.32	36.5

1) By elemental analysis.

2) By GPC measurement.

### 2.2. Bulk aggregation structure

To study bulk crystalline structure, wide angle X-ray diffraction (WAXD) measurement was carried out on a diffractometer (M18XHF Mac Science Ltd.) using monochromatic CuK $\alpha$  radiation with the wavelength of 0.154 nm, which was generated at 40 kV and 200 mA. Small-angle X-ray scattering (SAXS) was used to examine bulk phase-separated structure on a Rigaku RU-200 diffractometer with the same operating condition mentioned above. Besides, bulk phase-separated structure was observed by transmission electron microscopy (TEM) with a Hitachi H-7500 operated at accelerating voltage of 100 kV.

### 2.3. Surface aggregation structure and wetting properties

Surface aggregation states and wetting properties of the copolymers were studied by angular-dependent X-ray photoelectron spectroscopy (ADXPS) in conjunction with dynamic contact angle measurement. All measurements were made with the 200 nm-thick copolymer films, which were annealed at 423K for 24h, prepared on cleaned silicon wafers with native oxide layer. ADXPS measurement was carried out using a Physical Electronics 5800 spectrometer. Monochromatic Al K $\alpha$  was used for X-ray source. Fluorine atoms were easily damaged by X-ray exposure. Hence, the specimen was always cooled down during the measurement using liquid nitrogen. C<sub>1s</sub> peak corresponding to neutral carbon was assigned to a

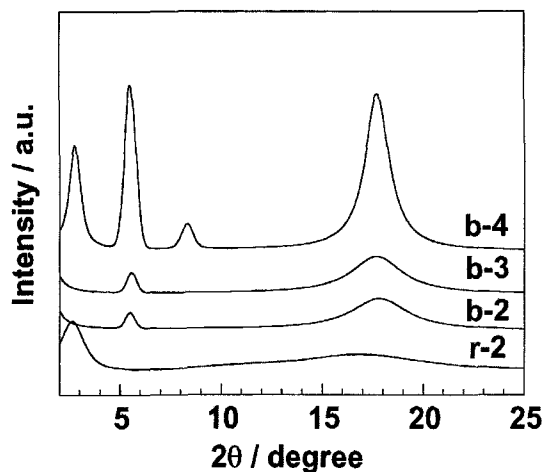


**Fig.2** WAXD profiles of diblock copolymers and random copolymer.

binding energy of 285.0 eV to correct for the charging energy shift. The analytical depth of XPS ( $d$ ) from the outermost surface is defined by  $3\lambda \cdot \sin \theta$ , where  $\lambda$  and  $\theta$  are inelastic mean-free path of photoelectrons in a solid and emission angle of photoelectrons, respectively. The inelastic mean-free path of photoelectrons was calculated by Ashley's equation <sup>4</sup>. The emission angle of photoelectrons was varied from 15° to 90° in this experiment. Dynamic contact angle for the copolymer films was measured by a sessile drop method using a Kyowa Kaimen Kagaku CA-A model apparatus. Water and dodecane were used as probe liquids.

## 3. RESULTS and DISCUSSION

### 3.1. Bulk aggregation structure

Fig.2 shows WAXD patterns of P(St-b-PFA) and P(St-*ran*-PFA) copolymers. The pattern of b-4 showed clear four diffraction peaks at  $2\theta = 17.9, 8.4, 5.6$  and  $2.9$ , corresponding to Bragg spacing of 0.50, 1.07, 1.58 and 3.16 nm. The spacing of 0.50, 1.58 and 3.16 nm are assignable to intermolecular distance between two adjacent side perfluoroalkyl chains, the side chain length and twice the side chain length <sup>5,6</sup>. At present, the Bragg spacing of 1.07 is tentatively thought as second order diffraction of the intermolecular distance between the side chains. Since the diffraction peak arisen from twice the side chain length is clearly observed, it seems likely that the perfluoroalkyl groups form a smectic-like layer structure in the bulk <sup>5,6</sup>. With decreasing PFA content, the diffraction peaks at  $2\theta = 8.4$  and  $2.9$  disappeared, as shown for the patterns of b-2 and b-3. In addition, the diffraction peak at  $2\theta = 17.9$  became broader and weaker as the PFA content decreased. These results show that the structure order for the P(St-b-PFA) copolymers decreased with decreasing PFA content. It should be here noted that the formation of smectic-like layer is only seen for b-4. And, for the P(St-*ran*-PFA), the structure order seems to be not so good.

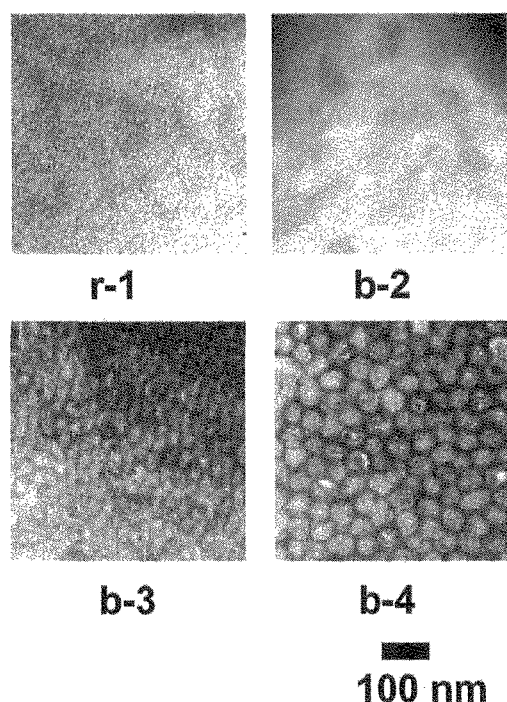


Fig.3 TEM images of diblock copolymers and random copolymer.

Fig.3 shows TEM images. In the case of b-3 and b-4, a microphase-separated structure with cylinders was clearly observed. Since the observation specimens were stained using  $\text{RuO}_4$ , PSt blocks were preferentially stained. Hence, darker regions in the TEM images denote the PSt blocks. On the other hand, a distinct microphase-separated morphology was not observed for b-2 and random copolymer.

For b-4, the thickness of PSt region and the diameter of a PFA domain were roughly estimated to be 10 and 40 nm, respectively. The domain spacing obtained from the TEM image for b-4 was larger than that for b-3. The domain identity periods for b-3 and b-4 estimated by SAXS measurement were  $29.7 \pm 9.4$  and  $40.6 \pm 1.8$  nm, respectively. The both results by TEM and SAXS are in agreement for each other with the experimental accuracy. In the next section, we focus on the surface aggregation structure of the P(St-*b*-PFA) films.

### 3.2. Surface aggregation structure and wetting properties

ADXPS is applied to the P(St-*b*-PFA) films to examine the distribution of perfluoroalkyl groups in the surface region. Fig.4 shows the atomic ratio of fluorine to carbon (F/C) as a function of  $\sin \theta$  corresponding to the analytical depth<sup>7</sup>. Smaller value of  $\sin \theta$  means shallower depth. In the case of P(St-*b*-PFA) films, the F/C increased with decreasing  $\sin \theta$ . And, all F/C values obtained by XPS were much higher than the bulk F/C one calculated from its chemical structure. These results make it clear that the perfluoroalkyl groups are enriched in the

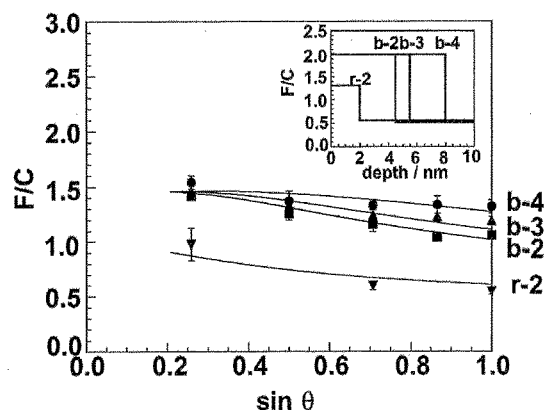


Fig.4 Sin  $\theta$  dependence of atomic ratio of fluorine to carbon (F/C) for diblock and random copolymer films as a function of PFA block content. The inset denotes model depth profiles of F/C to fit the experimental F/C-sin  $\theta$  relations.

outermost surface region. In the case of P(St-*ran*-PFA) film, the surface fluorine content was always lower than that of the P(St-*b*-PFA) film at a given  $\sin \theta$ , although slightly increased with decreasing  $\sin \theta$ . Interestingly, the values at a relatively larger  $\sin \theta$  were almost close to the bulk one. Hence, it is plausible that the surface segregation of perfluoroalkyl groups for the P(St-*ran*-PFA) film is not so remarkable in comparison with the diblock copolymers.

In XPS measurement, photoelectrons are not uniformly emitted from a given analytical depth region. Instead, the detected amount of photoelectrons exponentially decays with increasing depth, meaning that the relation of F/C value vs.  $\sin \theta$  cannot be simply regarded as the depth profile of fluorine. Hence, the real depth profile of F/C near the surface was tried to extracted on the basis of Paynter's analysis using experimental XPS data<sup>8</sup>. In this method, the surface region is first divided into compositionally uniform parallel layers. Since the intensity of photoelectrons from the multilayer can be given by Eq.(1), the real depth profile of F/C is supposed to be deduced

$$I(\theta, x) = Fk \left( \int_0^{x_1} \exp\left(-\frac{x}{\lambda \sin \theta}\right) n_1 dx + \int_{x_1}^{x_2} \exp\left(-\frac{x}{\lambda \sin \theta}\right) n_2 dx + \dots \right) \quad (1)$$

where  $n_i$  is the number density of atoms in a homogeneous layer from  $x_i$  to  $x_{i+1}$ . When the depth profiles shown in the inset of Fig.4 were assumed, the experimental data sets were best-fit, as drawn by the solid curves in the main panel of Fig.4. Invoking that the inset reflects real F/C-depth relations, it is conceivable that the fluoroalkyl layer are formed at the surface and its thickness is dependent on the PFA content. Also, the formation of the surface fluoroalkyl layer was not perfect for the P(St-*ran*-PFA) film. These are also confirmed by dynamic secondary ion mass spectroscopy.

To discuss about the wettability of the P(St-*b*-PFA) film surfaces, dynamic contact angle

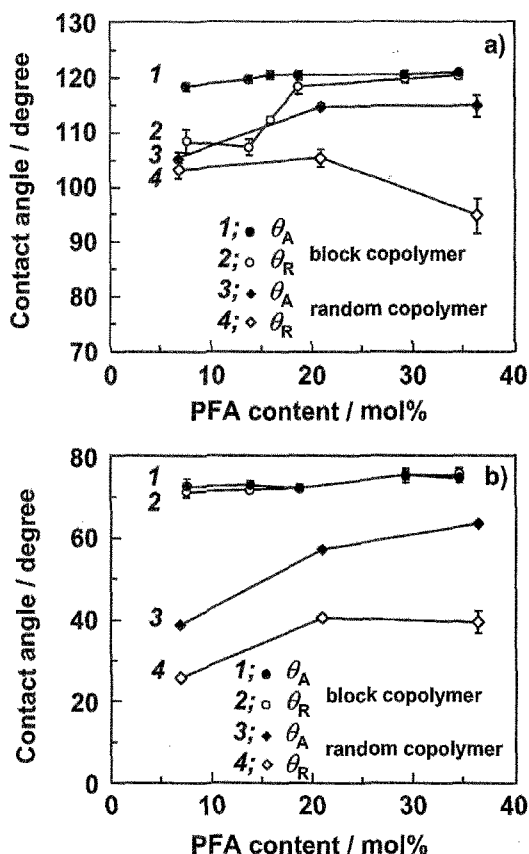


Fig.5 Dynamic contact angle vs. PFA content relation for diblock and random copolymer films. a) water and b) dodecane.

measurement was made using water and dodecane as probe liquids. In this case, contact angle hysteresis, defined by differences between advancing contact angle ( $\theta_A$ ) and receding contact angle ( $\theta_R$ ), can be accessible in addition to the contact angle value itself. Lower contact angle hysteresis means more excellent and stable liquid repellent property.

Fig.5 shows the relationship between dynamic contact angle and PFA content of the diblock copolymers; (a) to water and (b) to dodecane. For a comparison, the data for the P(St-*ran*-PFA) films are also plotted. Advancing contact angles to water monotonically increased with increasing PFA content and the values for the block copolymers were larger than those for random ones. Receding contact angle for the P(St-*b*-PFA) films was abruptly increased at around 15–20 mol%. This implies that the surface wettability for the P(St-*b*-PFA) films becomes more stable and excellent once the PFA content goes beyond 15–20 mol%. It should be interesting to combine the above with a fact that the structure order for the P(St-*b*-PFA) films drastically improved as the PFA content proceeds this value. In the case of the P(St-*ran*-PFA) films, the contact angle hysteresis was always larger than that of the corresponding P(St-*b*-PFA) film at all range. Such was remarkably seen for surface wettability to dodecane. Both advancing

and receding contact angles for the P(St-*b*-PFA) films monotonically increased with almost no contact angle hysteresis, and the hysteresis for the P(St-*ran*-PFA) films are large at all range, as shown in the part (b) of Fig.5.

#### 4. CONCLUSIONS

Well-defined poly(styrene-*block*-2-perfluooctyl ethyl acrylate) [P(St-*b*-PFA)] copolymers with various chemical compositions were synthesized by ATRP. Bulk and surface aggregation states in the films of P(St-*b*-PFA) were studied in detail by WAXD, SAXS, TEM and XPS measurements. The P(St-*b*-PFA) films with the PFA fraction higher than 20 mol% were in a highly-ordered microphase-separated state in bulk and at surface as well. For the P(St-*b*-PFA) films with highly-ordered structure, the surface smectic-like layer might prevent from reconstructing the surface structure. This would be the reason why the P(St-*b*-PFA) films with the PFA fraction higher than 20 mol% exhibited the intriguing liquid repellent properties.

#### 5. ACKNOWLEDGEMENT

We are most grateful for helpful discussion with Dr Hideaki Yokoyama, AIST. This study is carried out as 'Nanostructure Polymer Project' supported by NEDO (New Energy and Industrial Technology Development Organization) launched in 2001.

#### 6. REFERENCES

- [1] A. G. Pittman, "Fluoropolymers" p. 419, WILEY-INTERSCIENCE, New York, (1972).
- [2] J. Wang, G. Mao, C. K. Ober, and E. J. Kramer, *Macromolecules*, **30**, 1906 (1997).
- [3] K. Matyjaszewski and J. Xia, *Chem. Rev.*, **101**, 2921 (2001).
- [4] J. C. Ashley, *IEEE Trans Nucl Sci*, **NS-27**, 1454 (1980).
- [5] V. V. Volkov, N. A. Plate, A. Takahara, T. Kajiyama, N. Amaya, and Y. Murata, *Polymer*, **33**, 1316 (1992).
- [6] Y. Katano, H. Tomono, and T. Nakajima, *Macromolecules*, **27**, 2342 (1994).
- [7] K. Tanaka, D. Kawaguchi, Y. Yokoe, T. Kajiyama, A. Takahara, and S. Tasaki, *Polymer*, **44**, 4171 (2003).
- [8] R. W. Paynter, *Surf Interface Anal*, **3**, 186 (1981).

(Received October 29, 2003; Accepted November 25, 2003)